行政院國家科學委員會補助專題研究計畫成果報告

無序系統內局限與非局限態轉變之研究(2/2)

計畫類別：個別型計畫
計畫編號：NSC 94－2112－M－009－016
執行期間：94 年 8 月 1 日 至 95 年 7 月 31 日

計畫主持人：吳天鳴教授（交通大學物理研究所）
計畫參與人員:黃邦杰博士研究生(交通大學物理研究所)

成果報告類型： 完整報告

本成果報告包括以下應繳交之附件：

出席國際學術會議心得報告及發表之論文各一份

執行單位：國立交通大學物理研究所

中 華 民 國 96 年 1 月 17 日

從簡單液體的瞬間正則模的相鄰能階統計分析，我們檢驗在無序系統的中振動能譜內移動邊界的臨界性。簡單液體的瞬間正則模能譜是由 Hessian 矩陣的本征值所構成，而 Hessian 矩陣屬於歐幾里德亂數矩陣系集。在瞬間正則模能譜，有兩個移動邊界，一個是正本征值，一個是負本征值。在每一個移動邊界附近，臨界相鄰能階分佈與標準安德森模型所得到的分佈是一樣的。而在這兩個移動邊界，局限長度的臨界指數是不一樣的。

關鍵詞：侷限與非侷限態轉變、可動性邊界、安德森模型、向量歐幾里德隨機矩陣、態能階間距分佈

Criticality of mobility edges in vibrational spectrum of topologically disordered systems

B. J. Huang and Ten-Ming Wu *

Institute of Physics, National Chiao-Tung University, HsinChu, Taiwan 300, Republic of China

Jan 16, 2007

*Corresponding author: tmw@faculty.nctu.edu.tw

Abstract

By analyzing the nearest-neighbor level-spacing (LS) statistics of the instantaneous normal modes (INMs) in a simple fluid, we have examined the criticality of mobility edge (ME) in the vibrational spectra of topologically disordered systems. The INM spectrum of a simple fluid is the eigenvalues of the Hessian matrices, which are an ensemble of the Euclidean random matrices with elements subject to several constraints. The localtions of two MEs in the INM spectrum, with one in the branch of positive eigenvalues and the other in that of negative eigenvalues, are numerically determined by the scaling law for four finite sizes of the simple fluid. The critical LS distribution near each ME in the INM spectrum is almost identical with the one obtained from the Anderson model. However, the critical exponents of the localization lengths at the two MEs are found to be different.

PACS: 61.25.Mv, 63.50.+x, 61.20.Ne

I Introduction

Many universal properties at the localization-delcoalization (LD) transition, which is also termed as mobility edge (ME), in the eigenstate spectra of disordered systems has been studied for a long time [1, 2]. Anderson model (AM) of electron transport in a lattice [3] is one of the well-known models to study these universal properties, and many results of the AM at the LD transition have been given [4, 5, 6, 7, 8, 9]. In random-matrix theroy [10], the AM in three-dimensional space is classified as the Gaussian orthogonal ensemble (GOE), which consists of the real and symmetric matrix elements. For the AM with a disorder below some critical value, the spatially localized and delocalized (or extended) eigenstates, which are separated in different regions of the spectrum, are characterized by different level statistics [11]. For the delocalized eigenstates, any two nearest-neighbor energy levels are correlated due to the large overlap in the two eigenstates, and the distribution $P(s)$ of the nearest-neighbor level spacing (LS) is well approximated by the Wigner surmise $P_W(s) = (\pi/2)s\ exp(-\pi s^2/4)$ [12]. On the other hand, any two nearest-neighbor energy levels of the localized eigenstates are uncorrelated for the very small overlap in the two eigenstates, and $P(s)$ follows the Poisson distribution $P_P(s) = exp(-s)$. Generally, for a disordered system of a finite size, $P(s)$ in these two regimes are size-dependent, but vary in opposite tendency with the system size. According to the scaling theory of localization [13], at the boundary of the two regimes, which is the ME, the nearest-neighbor level statistics is size-independent and exhibits a universal behavior, charaterized by a critical nearest-neighbor LS distribution $P_C(s)$. This critical LS distribution has been studied numerically by examining the levels in the band center of the AM at a critical disoreder by varing the cubic size of a lattice from 5 up to 10^2 [8]. Though the precise formula of $P_C(s)$ depends on the boundary conditions of the lattice, $P_C(s)$ is generally linear in small s as the Wigner surmise; however, the asymtotics of $P_C(s)$ for large s is still an open question. The

size independence of $P_C(s)$ provides a special feature to determine the ME in the spectrum, in terms of examining the invariance of some quantity related to $P(s)$ as the system size is varied from small to large. Compared with other methods to determine the ME, this method benefits by only requiring the eigenvalues of the disordered system at several different system sizes; however, very large system sizes and a large amount of realizations for average have to be condisered.

Recently, harmonic vibrations in topologically disordered systems (liquids and glasses) have been received considerable attention [14, 15, 16]. The harmonic vibrations of a disordered system can be described by the Hessian matrices, which are the second-order derivatives of the potential energy of the system with respect to the particle displacements. For three-dimensional glasses, the vibrations near zero eigenvalue are generally extended in the space, but the vibrations in the tail of the spectrum are localized in space. Therefore, there is a sharp boundary, similar as the ME of the AM, to separate the two kinds of vibrational modes in the spectrum. The thermal conductivity of a glass, which is essentically determined by the extended vibrational modes, is strongly influenced by the location of the ME [17]. The location of the ME in a vibrational spectrum has been determined by the measures computed from participation numbers [18], Thouless criterion, multifractal analysis, LS statistics. There are two difficulties in determining the location of the ME in the vibrational spectra of glasses in three-dimensional space: One is the vector nature of vibrations, which largely increases the dimension of the Hessian matrices, and the other is the highly packing of particles in a glass, which makes the matrices non-sparse. These two features make numerically diagonalize the Hessian matrics of glasses very difficult, and the numerical determination of the ME in the vibrational spectra of the disordered systems without a lattice reference frame is still a challenge problem. In many studies, for simplicity, the vector vibrations in three-dimensional space have been reduced to scalar quantities or the disordered models are crystalline

systems with random masses or force constants, which make the Hessian matrices sparse.

The physical system we are going to study is the intantaneous normal modes (INMs) of a simple fluid [19]. Originally developed for describing the short-time dynamics, and recently extended to characterize the local topography of potential energy surface (PES), the instantaneous normal modes (INMs) of a fluid are defined as the eigenmodes of the Hessian matrices at the configurations along the evolution of the system, and the INM spectrum provides the information in regard to the local-curvature distribution of the PES [20, 21]. Due to the vector nature of particle displacements in three-dimensional space, the Hessian matrices of a fluid are composed of 3×3 blocks [22, 23], which are functions of the relative distances of particle pairs. So, the matrices can be recognized as a generalized version of the Euclidean random matrices, with randomness originating from the disorder of particle positions in the configuration ensemble [24]. Compared with the GOE in random-matrix theory [10], the real symmetric elements of a Hessian are subject to the following constraints due to physical considerations [25]: (I) sum rules between the diagonal and off-diagonal blocks because of momentum conservation for vibrations, (II) triangle rule for the relative positions of any three particles [26], which makes only $N-1$ off-diagonal blocks of each Hassian independent with N being the number of particles, and (III) the internal constranints between the elements of each off-diagonal block. None of these constraints appear in the AM. The constraints due to the triangle rule are ignored in those random models with a reference of lattice and the constraint III do not appear in the scalar-vibration models. [14, 27, 28].

In this paper, we investigate the ME in the INM spectrum of a truncated Lennard-Jones (TLJ) fluid at reduced density $\rho^* = 0.972$ and reduced temperature $T^* = 0.836$ in the Lennard-Jones (LJ) reduced units [29, 30]. The TLJ potential, which is only the repulsive port of the LJ potential, is obtained by truncating out

the LJ potential at the minimum and then lifting up with an amount of the depth of the minimum. Due to the short-range nature of the TLJ potential, the Hessian matrices of the TLJ fluid are sparse and diagonalized with the Lanczcos method. The configurations of the TLJ fluid were generated by Monte Carlo simulations. Presented in Fig. 1 is the eigenvaule spectrum $D(\lambda)$ of the Hessian matrices of the TLJ fluid, with the spectrum being normalized and for each configuration the three eigenvalues of zero due to the contraint I neglected. Unlike the symmetric spectrum of the AM, the spectrum shown in Fig. 1 is quite asymmetric, and cosists of two branches with positive and negative eigenvalues, which we will consider separately. In each branch, the eigenvectors with small eigenvalues are extended in space, but those of the eigenvalues in the tail of the spectrum are localized in space. Thus, there is a ME in each branch.

To analyze the level statistics of eigenmodes with eigenvalues λ_i in a range from λ_1 to λ_2, we first unfold these eigenvales with the following procedure [31]

$$z_i = \frac{1}{D_0} \int_{\lambda_1}^{\lambda_i} D(\lambda) d\lambda, \tag{1}$$

where the normalization factor $D_0 = \int_{\lambda_1}^{\lambda_2} D(\lambda) d\lambda$ is the total density of eigenmodes between λ_1 and λ_2. The unfolded eigenvalue z_i is a variable from zero to one. By analyzing the eigenvalue spectrum of the TLJ fluid with smaller number of particles, we find that the two MEs fall into the ranges $\lambda = 1150 \sim 1230$ and $\lambda = -95 \sim -80$ for the positive- and negative-eigenvalue branches, respectively. Shown in the insets of Fig. 1 are the unfolding procedures of the eigenvalues in each of the two ranges with the unfolded variables z_p and z_n for the positive and negative branches, respectively.

In the study of the vibrational modes of percolation clusters [32], an investigated quantity related to $P(s)$ is $I_N =< s^2 > /2$, where $< s^2 >= \int_0^\infty s^2 P(s) ds$ is the second moment of $P(s)$. $I_N = 2/\pi$ for the Wigner's surmise, and $I_N = 1$ for the

Poisson distribution. Generally, for a disordered system of finite size, I_N increases monotonously from $2/\pi$ to 1 with from the regime of extended eigenstates to that of localized ones. However, the function of I_N depends on the system size: With increasing the system size, I_N increases in the regime of localized eigenstates, but decreases in that of delocalized eigenstates. The value of I_N is invariant with the system size only at a transition point, where the ME is located.

For $\lambda = 1150 \sim 1230$, we further divide equally the unfolded eigenvalues into eight sections. For each section, we define the nearest-neighbor LS as $s_i = (z_{i+1} - z_i)/\Delta$ [33], where Δ is the mean level spacing of the unfolded eigenvalues considered. The nearest-neighbor LS distribution $P(s)$ of these unfolded eigenvalues is defined by the condition that $P(s)ds$ is the probability to find the next eigenvalue at a distance between s and $s+ds$. Thus, $P(s)$ is normalized and its mean is unit. With the $P(s)$ of each section, the value of I_N is evaluated. For the eight sections, I_N as a function of the unfolded variable z_p is indicated by the symbols in Fig. 2A for four system sizes with N varied from 3000 to 24000. The similar results for $\lambda = -95 \sim -80$ are given in Fig. 2B. The numerical results in our calculations are summarized in Table I.

Apparently, the results of our calculation for I_N in Fig. 2 is generally consistent with the scaling law for the finite-size system. According to the scaling law, I_N has a solution of the form

$$I_N(z) = f(L/\xi), \tag{2}$$

where $f(x)$ is a function of one parameter, which is a ratio of the system size L of a finite system to the correlation length ξ of the infinite system. L is proportional to $N^{1/3}$. ξ is a function of the unfolded variable and divergent at the ME with a critical exponent ν as the following

$$\xi(z) = C(z - z_c)^{-\nu}, \tag{3}$$

where C is some constant. Close to the ME, the one-parameter function $f(x)$ is expanded into a Taylor series. Up to the third order of the expansion, $I_N(z)$ can be expressed as

$$I_N(z) = I_c + a_1\big[(z - z_c)N^{1/3}\big]^{1/\nu} + a_2\big[(z - z_c)N^{1/3}\big]^{2/\nu} + a_3\big[(z - z_c)N^{1/3}\big]^{3/\nu}. \quad (4)$$

With I_c, z_c, a_1, a_2, a_3 and ν being the fitting parameters, we use this equation to fit the numerical data of the four system sizes in Fig. 2. The results are indicated by the solid lines in Fig. 2. with the parameters given in Table II. The MEs in the two branches occur at the unfolded variables z_{pc} and z_{nc}, which correspond to the eigenvalues $\lambda_{pc} = 1184.2$ and $\lambda_{nc} = -86.6$, respectively. Acording to our results, the two critical exponents ν_p and ν_n of the MEs in the positive- and negative-eigenvalue branches are somewhat different, with $\nu_p = 1.74$ but $\nu_n = 1.57$, which is almost equal to the critical exponent of the AM.

We define a new function

$$h(\eta) = \frac{I_N(z) - I_c}{a_1} \quad (5)$$

with the scaling parameter $\eta = \xi N^{-1/3}$. At the ME, η is divergent and the value of the h function is zero. The positive and negative values of the h function correspond to the localized and extended regimes, respectively. For each branch, the numerical data of the h function for the four system sizes collapse onto a single scaling fucntion as shown in Fig. 3. Near the ME, the scaling functions of the two branches are almost identical; this uniqueness in the single scaling function is due to the second term on the right hand side of Eq. (4). However, as deviated from the ME with the scaling parameter η less than *one*, the two scaling functions are no longer conincident with each other, because of the different nonlinearity of the I_N function in Eq. (4) for the two branches.

To examine the critical LS distribution at the ME, we select the eigenvalues in two narrow intervals $\lambda = 1182 \sim 1188$ and $\lambda = -88 \sim -85$, in which the MEs in

the positive and negative branches are contained, respectively. For the realizations generated by our simulations, the number of the LS for the selected eigenvalues in the two interval are roughly 6×10^5 for each system size. Indicated by the numerical data of the four system sizes in Fig. 4, the LS distributions of the eigenvalues in the two intervals are in general size-independent. Also, the numerical data in Fig. 4 can be well fitted by the following formula

$$P_c(s) = \frac{A_c^2 \ s \ \exp\left(\mu - \sqrt{\mu^2 + (A_c \ s)^2}\right)}{\sqrt{\mu^2 + (A_c \ s)^2}}, \tag{6}$$

with A_c and μ being the fitting parameters. The results of the fitting are shown by the solid lines in Fig. 4, with $A_c = 1.8827$ and $\mu = 1.5446$ for the positive branch and $A_c = 1.8708$ and $\mu = 1.5336$ for the negative branch. Within numerical errors, both LS distributions shown in Fig. 4 are close to the critical LS distribution obtained from the AM. This is consistent with the universality of the critical LS distribution. For small s, the critical LS distribution is linearly proportional to s as the Wigner surmise $P_W(s)$. For large s, the fitting formula in Eq. (5) becomes Poisson-like and decays exponentially with a decay rate A_c. However, we should give a notice that the numerical data of the LS distribution for large s, plotted in logarithmic scale in the insets of Fig. 4, are widely spread due to the limitation of a finite-size system for numerical calculation. Therefore, the precise behavior of the critical LS distribution for large s is still an open question.

In this report, we have investigated the universality of the LS statistics at the LD transition in the vibrational spectrum of a topologically disordered system which does not possess a lattice reference. The LD transition, also referred as the ME, is the boundary of the localized and delocalized eigenstates in the spectrum. The disordered system we study is the TLJ fluid, and the vibrational spectrum of the disordered system is the eigenvalues of the Hessian matrices, which are an ensemble of Euclidean random matrices. The vibrational spectrum of the TLJ fluid consist of

two branches with positive and negative eigenvalues, with one ME in each branch. According to the scaling law, the universal behavior at the mobility edge should be size-independent. We have calculated the second moments of the LS distributions for four system sizes with particle numbers from 3000 to 24000. With the size indepnedence on the LS distribution, the two mobility edges in the vibrational spectrum of the TLJ fluid are found. Through a fitting for the second moments of the four system sizes with a scaling function of one parameter, we find the critical exponent of the correlation length, which diverges at the ME, to be 1.57 for the negative-eigenvalue branch and 1.74 for the positive-eigenvalue branch. The LS distribution near any one of the mobiltiy edge agrees within the numerical errors with the critical LS ditribution obtained from the AM. This confirms the universality of the LS statistics at the LD transition.

References

[1] M. Janssen, Phys. Rep. **295**, 1 (1998).

[2] A. D. Mirlin, Phys. Rep. **326**, 259 (2000).

[3] P. W. Anderson, Phys. Rev. **109**, 1492 (1958).

[4] S. N. Evangelou and E. N. Economou, Phys. Rev. Lett. **68**, 361 (1992).

[5] B. I. Shklovskii, B. Shapiro, B. R. Sears, P. Lambrianides, and H. B. Shore, Phys. Rev. B **47**, 11487 (1993).

[6] E. Hofstetter and M. Schreiber, Phys. Rev. B **48**, 16979 (1993); **49**, 14726 (1994).

[7] S. N. Evangelou, Phys. Rev. B **49**, 16805 (1994).

[8] I. K. Zharekeshev and B. Kramer, Phys. Rev. Lett. **79**, 717 (1997).

[9] F. Milde, R. A. Romer, and M. Schreiber, Phys. Rev. B **61**, 6028 (2000).

[10] M. L. Mehta,*Random Matrices* (Academic Press, San Diego, 1991).

[11] J. M. Ziman,*Models of disorder* (Cambridge University Press, London, 1979).

[12] E. P. Wigner, Ann. Math. **53**, 36 (1951); **62** 548 (1955); **65**, 203 (1957); **67** 325 (1958).

[13] P. Sheng, *Introduction to Wave Scattering, Localization, and Mesoscopic Phenomena* (Academic Press, San Diego, 1995)

[14] W. Schirmacher, G. Diezemann, and C. Ganter, Phys. Rev. Lett. **81**, 136 (1998).

[15] S. N. Taraskin, Y. L. Loh, G. Natarajan, and S. R. Elliott, Phys. Rev. Lett. **86**, 1255 (2001).

[16] T. S. Grigera, V. Martin-Mayor, G. Parisi, and P. Verrocchio, Phys. Rev. Lett. **87**, 085502 (2001).

[17] X. Yu and D. M. Leitner, Phys. Rev. B **74**, 184305 (2006).

[18] B. B. Laird and H. R. Schober, Phys. Rev. Lett. **66**, 636 (1991); H. R. Schober and B. B. Laird, Phys. Rev. B **44**, 6746 (1991).

[19] R. M. Stratt, Acc. Chem. Res. **28**, 201 (1995).

[20] T. Keyes, J. Phys. Chem. **101**, 2921 (1997).

[21] W. X. Li, T. Keyes, R. L. Murry, and J. T. Fourkas, J. Chem. Phys. **109**, 9096 (1998).

[22] T. M. Wu and R. F. Loring, J. Chem. Phys. **97**, 8568 (1992).

[23] Y. Wan and R. M. Stratt, J. Chem. Phys. **100**, 5123 (1994).

[24] M. Mèzard, G. Parisi, and A. Zee, Nucl. Phys. B **559**, 689 (1999).

[25] W. J. Ma, T. M. Wu, and J. Hsieh, J. Phys. A: Math. Gen. **36**, 1451 (2003).

[26] D. A. Parshin and H. R. Schober, Phys. Rev. B **57**, 10232 (1998).

[27] Y. Akita and T. Ohtsuki, J. Phys. Soc. Jpn **67**, 2954 (1998).

[28] J. W. Kantelhardt, S. Russ, and A. Bunde, Phys. Rev. B **63**, 064302 (2001).

[29] T. M. Wu, W. J. Ma, and S. F. Tsay, Physica A **254**, 257 (1998).

[30] T. M. Wu, W. J. Ma, and S. L. Chang, J. Chem. Phys **113**, 274 (2000).

[31] S. Sastry, N. Deo, and S. Franz, Phys. Rev. E **64** 016305 (2001).

[32] J. W. Kantelhardt, A. Bunde, and L. Schweitzer, Phys. Rev. Lett. **81**, 4907 (1998).

[33] G. Fagas, V. I. Fal'ko, C. J. Lambert, and Y Gefen, Phys. Rev. B **61**, 9851 (2000).

Figure Captions

Fig. 1 - Density of eigenvalues $D(\lambda)$ for the Euclidean random matrices of the TLJ fluid at $\rho^* = 0.972$ and $T^* = 0.836$. The eigenvalues λ are in unit of $\epsilon/m\sigma^2$, where m is the particle mass. The two insets show the unfolding procedures of the eigenvalues in two separated ranges in which the mobility edges are contained: (a) for λ between 1150 and 1230 and (b) for λ between -95 and -80.

Fig. 2 - The size-dependent second moment I_N of the LS distribution as a function of the unfolded eigenvalue: z_r for (a) and z_i for (b). I_N is dependent on the system particle number N, which is varied from 3000 to 24000. The symbols stand for the results of the numerical calculations and the standard deviation of each data point is smaller than the size of the symbol. The solid lines are the results of the fitting equation for the four different system sizes with the fitted parameters given in Table II.

Fig. 3 - Scaling function $I_N - I_c)/a_1$ as a function of the scaling parameter $N^{-1/3}\xi$. The zero value of the scaling function is the mobility edge, and the positive and negative values correspond to the localized and extended regimes, respectively. The symbols are the numerical data for different system sizes. The solid line is the result of the fitting function $I_N = f(N^{-1/3}\xi)$ calculated for the positive eigenvalues with the parameters given in Table II, and the dashed line is the result calculated for the negative eigenvalues.

Fig. 4 - Level-spacing distribtuion $P(s)$ at the mobility edge in the positive-eigenvalue regime. The symbols stands for the numerical data of system sizes varied from $N = 3000$ to $N = 24000$. The solid line is the fitting result for these numerical data by the Eq. (3) with the fitting parameters.

Fig. 1

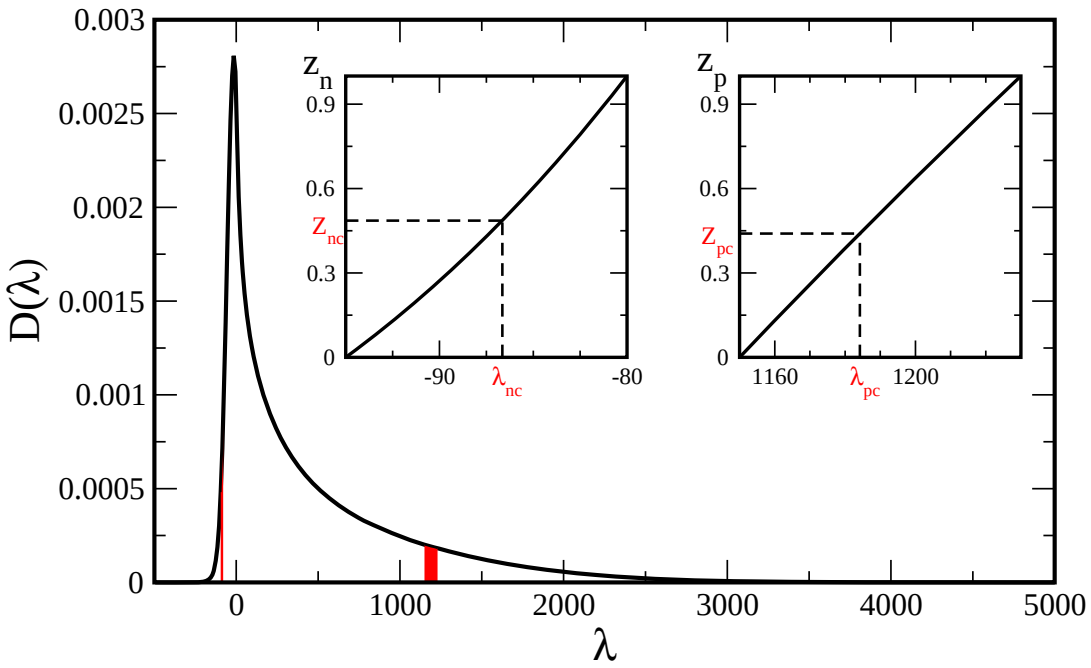
0.003
0.0025
0.002
0.0015
0.001
0.0005
0
D(λ)
0
1000
2000
3000
4000
5000
λ
z_n
0.9
0.6
Z_nc
0.3
0
-90
λ_nc
-80
z_p
0.9
0.6
Z_pc
0.3
0
1160
λ_pc
1200

Fig. 2A

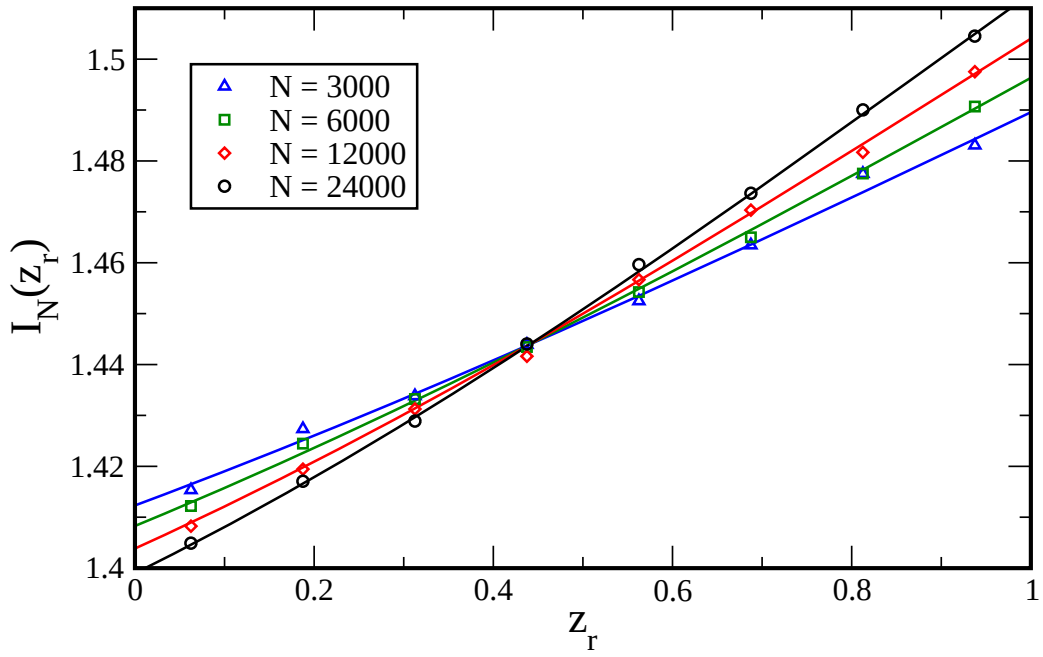
N = 3000
N = 6000
N = 12000
N = 24000
1.5
1.48
1.46
1.44
1.42
1.4
0
0.2
0.4
0.6
0.8
1
$I_N(z_r)$
z_r

Fig. 2B

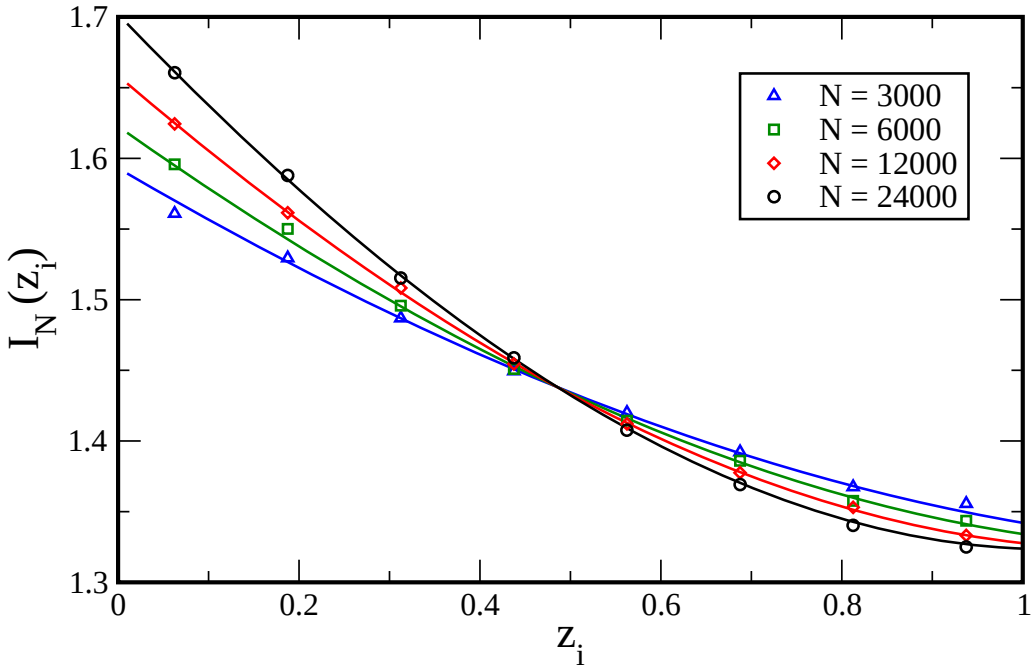

Fig. 3

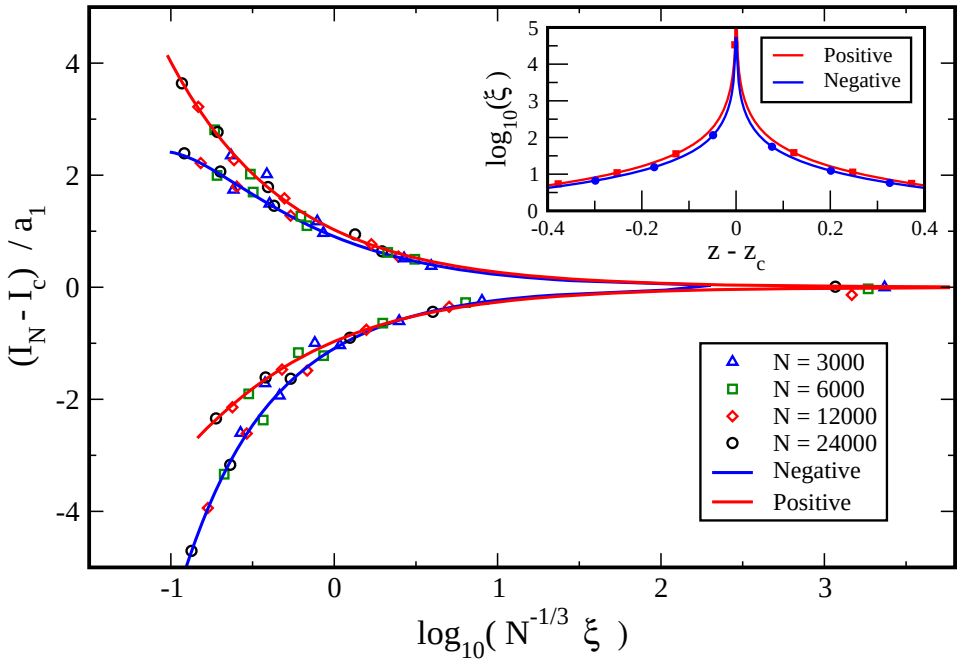
$(I_N - I_c) / a_1$
$\log_{10}(N^{-1/3} \xi)$
N = 3000
N = 6000
N = 12000
N = 24000
Negative
Positive
$\log_{10}(\xi)$
$z - z_c$
Positive
Negative

Fig. 4A

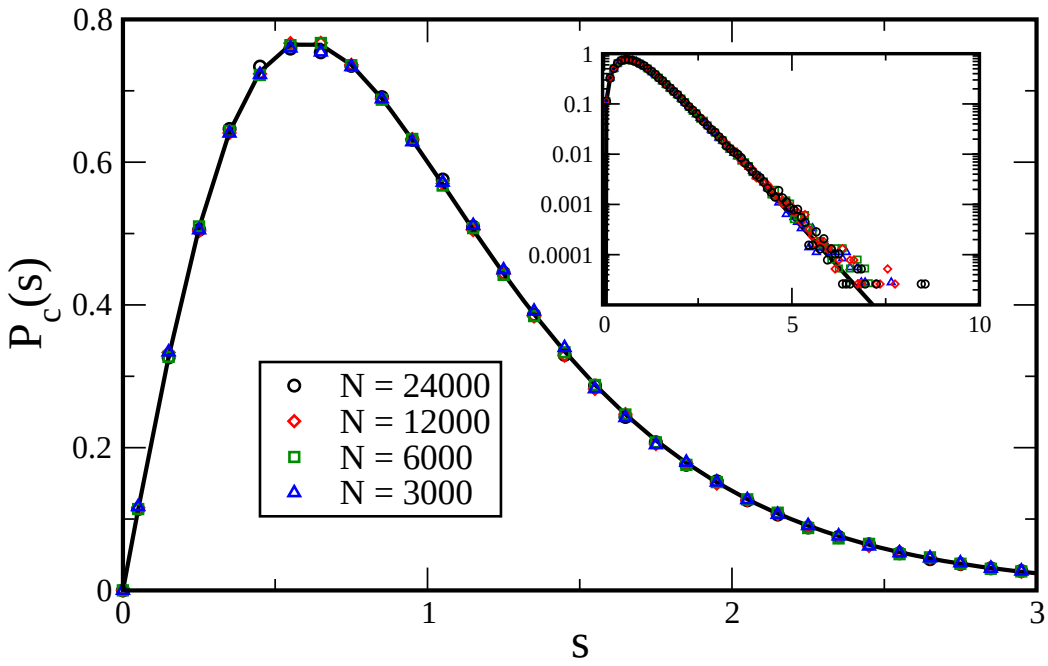
0.8
0.6
0.4
0.2
0
0
1
2
3
s
P_c(s)
N = 24000
N = 12000
N = 6000
N = 3000
1
0.1
0.01
0.001
0.0001
0
5
10

Fig. 4B

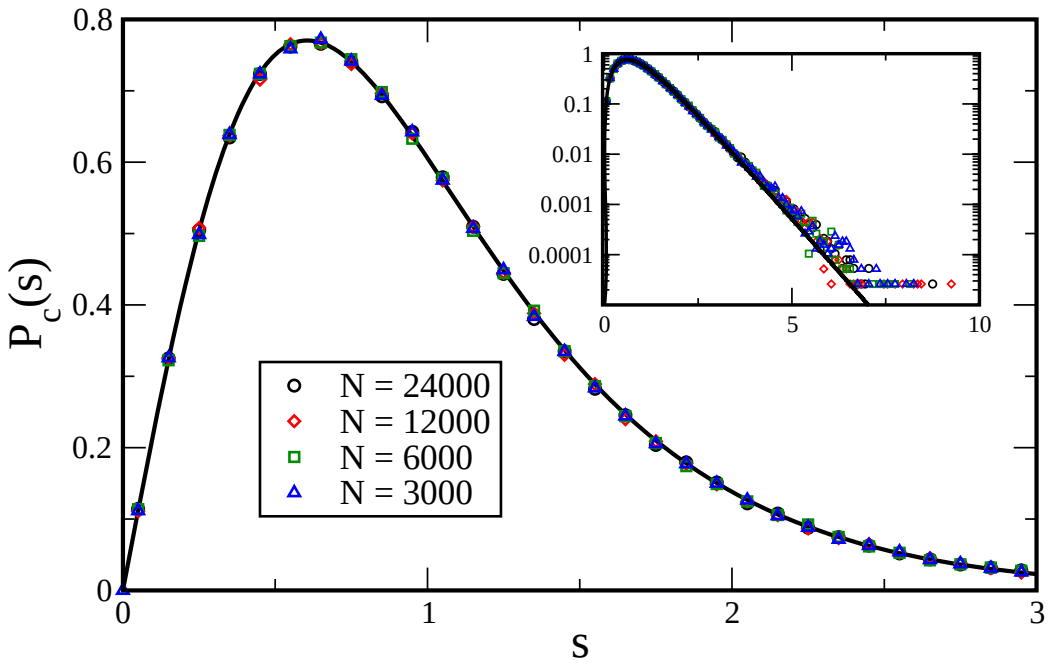
0.8
0.6
0.4
0.2
0
0
1
2
3
s
P_c(s)
N = 24000
N = 12000
N = 6000
N = 3000
1
0.1
0.01
0.001
0.0001
0
5
10

Table I. Numerical parameters of the eigenvalues λ in the range for various system sizes: N: number of particles; L: box length of the cubic system in unit of σ; M: number of samples; N_s: total number of level spacing; Δ: mean level spacing; $D_0=(3N\Delta)^{-1}$: integrated density of states in the eigenvalue range

		λ from 1150 to 1230				λ from -95 to -80			
N	L (σ)	M	$N_s\times10^{-6}$	$\Delta\times10^{3}$	$D_0\times10^{2}$	M	$N_s\times10^{-6}$	$\Delta\times10^{3}$	$D_0\times10^{2}$
3000	14.56	64000	8.826	7.2	1.54	32000	3.052	1.05	1.057
6000	18.35	32000	8.823	3.6	1.54	16000	3.051	0.52	1.059
12000	23.12	16000	8.824	1.8	1.54	8000	3.050	0.26	1.059
24000	29.12	8000	8.824	0.9	1.54	4000	3.041	0.13	1.059

Table II. Parameters in Eq. (1) used to fit the numerical data in Fig. 2 for I_N of different system sizes and χ^2 is the estimated error of the fitting.

λ	I_c	z_c	$a_1\times10^{2}$	$a_2\times10^{3}$	$a_3\times10^{4}$	ν	$\chi^2\times10^{4}$
1150 ~ 1230	1.444	0.44	1.665	0.48	-0.45	1.74	0.41
-95 ~ -80	1.438	0.486	-4.73	4.41	1.0	1.57	2.5